HHS Public Access

Author manuscript

Brain Struct Funct. Author manuscript; available in PMC 2016 January 23.

Published in final edited form as:

Brain Struct Funct. 2016 January ; 221(1): 665–678. doi:10.1007/s00429-014-0932-4.

Developmental guidance of the retroflex tract at its bending point involves *Robo1-Slit2* mediated repulsion

Juan A. Moreno-Bravo[1], **Jesus E. Martinez-Lopez**[1], **M. Pilar Madrigal**[1], **Minkyung Kim**[2], **Grant S. Mastick**[2], **Guillermina Lopez-Bendito**[1], **Salvador Martinez**[1], and **Eduardo Puelles**[1]

[1]Instituto de Neurociencias de Alicante, Universidad Miguel Hernández-CSIC, 03550 Sant Joan d'Alacant, Alicante, Spain

[2]Department of Biology, University of Nevada, Reno, NV 89557, USA

Abstract

The retroflex tract contains medial habenula efferents that target the hindbrain interpeduncular complex and surrounding areas. This tract displays a singular course. Initially, the habenular axons extend ventralwards in front of the pretectum until they reach the basal plate. Next, they avoid crossing the local floor plate, sharply changing course caudalwards (the retroflexion alluded by the tract name) and navigate strictly antero-posteriorly across basal pretectum, midbrain and isthmus. Once they reach rhombomere 1, the habenular axons criss-cross the floor plate several times within the interpeduncular nuclear complex as they innervate it. Here we explored in vitro the timing and details of growth phenomena as these axons first change course, and examined the corresponding molecular background. The first dorsoventral course apparently obeys Ntn1 attraction. The decision to bend caudalwards next to the repelling thalamic floor plate seems related to Slit2 repulsive cues. We checked the role of local floor plate signaling by studying *Gli2* knockout mice. We found reduced expression of the *Slit* repulsive cues, suggesting involvement of the floor-derived *Robo-Slit* system in the normal guidance of this tract. The *Gli2−/−* phenotype caused a contralateral projection of most habenular axons, plus ulterior bizarre navigation rostralwards. Using *Slit* and *Robo* mutant mice, and open neural tube and co-culture assays, we determined that a *Robo1-Slit2* interaction is specifically required for impeding that habenular axons cross the thalamic floor plate. This pathfinding mechanism is essential to establish the functionally important habenulo-interpeduncular connection.

Keywords

Habenula; retroflex tract; Robo-Slit; axon guidance

Correspondence should be addressed to: Dr. Eduardo Puelles, Instituto de Neurociencias de Alicante, Universidad Miguel Hernández-CSIC, 03550 San Juan, Alicante, Spain. epuelles@umh.es.

Competing interests

The authors declare no competing financial interests.

Author Contributions

J.A.M-B and E.P designed research, J.A.M-B, J.E.M-L, M.P.M and M.K. performed research, G.L.-B, G.S.M and S.M contribute unpublished reagent/analytic tools and discussed results J.A.M-B and E.P analyzed results and wrote the manuscript.

Introduction

The habenula (Hb) consists of medial and lateral nuclei (mHb, lHb; Andres et al., 1999), found at the dorsal part of the alar plate of prosomere 2 (p2; Puelles and Rubenstein, 2003; Puelles et al., 2012). The Hb receives inputs from the basal forebrain via the stria medullaris, and projects to the midbrain and prepontine hindbrain (isthmus and rhombomere 1) through the retroflex tract (rft) (Sutherland, 1982; Morgane et al., 2005). The mHb axons mainly innervate the interpeduncular nucleus (IP), which they do by zig-zagging several times across the r1 floor plate (Ramon y Cajal, 1909 –Vol.I). The lHb axons innervate various target nuclei in the midbrain (VTA; SNC) and the rostral hindbrain (e.g., the rostromedial tegmental nucleus and the dorsal raphe nucleus; Bianco and Wilson, 2009). This system is a highly conserved pathway in all vertebrates; it connects the limbic forebrain with rostral hindbrain areas that participate in diffuse projection systems or their regulation, and is implicated in a range of functions (Sutherland, 1982; Klemm, 2004; Lecourtier and Kelly, 2007; Hong and Hikosaka, 2008, Hong et al., 2011). This circuitry is involved in control of the dopamine and serotonin systems, circadian rhythms, aversive responses, psychosis, reproduction and maternal behavior, cognition and regulation of sleep (Bianco and Wilson, 2009; Geisler and Trimble, 2008; Viswanath et al., 2014). Subtle alterations in the wiring of this system might account for some human pathophysiological conditions. Surprisingly, despite our abundant functional knowledge about this circuit, the development of the rft, the main efferent projection of the Hb, is still incompletely understood. This information is of interest to better understand the hypothetical malformations or dysfunctions of this system.

The rft has a singular and unique trajectory. The habenular axons extend from the dorsal alar p2 to the ventromedian part of r1 (Puelles and Rubenstein, 2003). They do this by travelling first along the dorsoventral dimension of the caudal thalamic region (just rostrally to the thalamo-pretectal or p1/p2 boundary) and the subjacent thalamic tegmentum; curiously, they do not continue to penetrate and cross the local floor plate, and instead turn caudalwards into a rostrocaudal course across the medial pretectal and midbrain tegmentum (basal plate) into the rostral hindbrain (isthmus and r1), always just outside the floor plate. Note the rft path has often been misinterpreted as stretching straightly from the habenula into the interpeduncular nuclei, without any bend; this error is partly due to the circumstance that the hairpin ventral bend of the cephalic flexure that deforms the mes-diencephalic territory masks the retroflexion of the habenulo-interpeduncular tract. The cited trajectory implies several key pathfinding decisions.

The first step, that gives rise to a tight fasciculated rft tract running dorsoventrally in front of the caudal limit of p2, is well known. At least two repulsive effects and one attractive cue are postulated that orient the dorsoventral initial growth of the pioneering axons and prevent the axons from dispersing into the p1 or p2 alar plates. The repulsion from alar p1 is mediated by local interaction of Neuropilin2 (Npn2) with Semaphorin3F (Sema3F; Funato et al., 2000; Sahay et al., 2003). In addition, interaction of Sema5A with heparan and chondroitin sulfate proteoglycans promotes the fasciculation of the rft tract and causes a repulsive effect that restrains the developing axons from penetrating other parts of the p2 alar plate (Kantor et al., 2004). Finally, Netrin1 (Ntn1) is an attractive cue released by the basal plate that promotes ventralward growth of the rft axons along the remaining

permissive route via its main receptor, Deleted in Colorectal Cancer (DCC; Funato et al., 2000). However, these mechanisms do not account for the complete trajectory of the rft. Other signaling cues must prevent the crossing of the p2 midline floor and redirect the axons to turn (retroflex) and navigate caudalwards across p1 and midbrain, in order to reach the target nuclei in the rostral hindbrain. The diencephalic floor plate is known to secrete different signals active in axonal guidance (Colamarino and Tessier-Lavigne, 1995; Tessier-Lavigne and Goodman, 1996; Kaprielian et al., 2001). The main molecules identified so far are Ntn1 (Kennedy et al., 1994), Slits (Long et al., 2004) and Semaphorins (Zou et al., 2000). The *Robo/Slit* signaling mechanism generally participates in midline repulsion of many axonal systems such as commissural axons (Long et al., 2004), pioneering longitudinal axons (Farmer et al., 2008; Devine and Key, 2008; Kastenhuber et al., 2009; Kim et al., 2011; Zhang et al., 2012) and various other axonal projections in the forebrain (Lopez-Bendito et al., 2007; Bagri et al., 2002; Plump et al., 2002; Ricaño-Cornejo et al., 2011).

The aim of this report was to describe in detail the embryonic development of the rft, focusing experimentally on the pathfinding decision taken by its pioneering axons where they change from their initial dorsoventral course into a caudalward trajectory. We analyzed the role of floor-plate signals in this navigational behavior, focusing our analysis on the *Robo-Slit* signaling mechanism and its presumable role in the investigated phenomenon.

Results

Trajectory of the rft in the adult brain and embryonic development

We first re-examined the trajectory of the rft in the adult mouse, since a description based on the prosomeric model was not available, and several sources in the literature hold that the course is straight from the habenula into the interpeduncular nucleus. We used the transgenic line *Pou4f1*-tauLacZ mouse as a model (Quina et al., 2005) to label with X-gal the habenular neurons and their axons in the rft (Fig. 1A). Our material corroborated that the habenular axons extend strictly dorsoventrally, caudally within prosomere 2, across its alar and basal plates, always in front of the p1/p2 or thalamo-pretectal boundary. Once they arrive at the p2 basal plate, they turn 90 degrees, and thereafter navigate adjacent to the floor plate in a caudal direction, crossing p1 and the midbrain, isthmus and r1, where terminal arborization occurs (see below).

In order to analyze in more detail the course of these axons when approaching the floor plate, we also labeled simultaneously the two habenular complexes. In an E18.5 embryo, we marked the right habenula with DiI (red signal) and the left habenula with DiA (green signal). In this way we compared the trajectories and projections of the two tracts (Fig. 1B–E). The tightly fasciculated habenular axons travelled ventrally (Fig. 1B), with the mHb axons occupying the core and the lHb axons the shell of the rft (Bianco and Wilson, 2009). When they arrived at the proximity of the floor plate, both tracts flattened and bent caudalward ipsilaterally (Fig. 1C). We noted that the mHb axons remain fasciculated close to the pial surface, while the lHb axons were less fasciculated and coursed in a deeper location. As they arrived at their targets, the lHb innervated the mesencephalic ventral tegmental area and substantia nigra pars compacta, as well as the rostral hindbrain raphe

nuclei, the dorsal and ventral tegmental nuclei, the rhabdoid nucleus and the rostromedial tegmental nucleus (Fig. 1D, E). The mHb axons crossed and re-crossed the r1 floor plate as they innervated the IP nucleus (Fig. 1D, E). Finally, some lHb axons projected rostrally into the hypothalamus, as described by Kiss et al. (2002). We schematically summarized in Figure 1F the trajectory of the rft. Three main navigational decision points are emphasized: sorting out of the habenula, change of course next to the p2 floor plate (not crossing the midline), and identifying selective terminal targets (Fig. 1F).

Therefore, during embryonic development the rft axons must use precise pathfinding information at least at three points to fulfill their trajectories. We analyzed sequential stages of development to determine the precise timing by which the axons make these navigational decisions. We studied the distribution of the DCC receptor, which appears strongly expressed in the mHb and weakly expressed in the lHb, and prepared open neural tube explants (ONTs) with the Hb labeled with either DiI or DiA tracers. We detected the first habenular axons in the proximity of the basal plate at E11.5 (arrow in Fig. 2A). DiI-labeled ONTs showed pioneering axons contacting the floor plate at this stage (Fig. 2B, B′). One day later, the pioneering axons increased in number, and contacted the floor plate (Fig. 2C). However, the DiI labeling revealed that the axons do not enter the floor plate, but instead modified their trajectory, orienting towards caudal territories (Fig. 2D, D′). At E13.5 the tract appeared much thicker (Fig. 2E), was clearly fasciculated and most of its fibers uniformly bend caudalwards (Fig. 2F, F′). Surprisingly, some scattered axons crossed the floor plate and joined the contralateral tract at this stage (arrows in Fig. 2F′).

Aberrant trajectory of the rft in the *Gli2* mutant

Our descriptive observations suggest that the floor plate probably releases or contains navigation cues that help the rft to change its earlier dorsoventral course into a rostrocaudal one. The pioneering axons closely approach and even contact the floor plate but do not enter it and turn caudalwards. With the aim to understand the role of the floor plate, we analyzed the phenotype of the *Gli2* mutant. This mutant fails to develop a floor plate due to alteration of *Shh* signaling, so that the ventral midline is formed by basal plate-like structures (Ding et al., 1998; Matise et al., 1998; Farmer et al., 2008). In contrast with the wt situation, we found that both rf tracts contact and merge in the abnormal basal plate midline in a E18.5 *Gli2* mutant brain (Fig. 3A, C). Strikingly, the resulting fiber bundle bent rostralward and ended in the rostral hypothalamus after crossing several times the midline (Fig. 3A). We noted that the mixing of both rft seemed asymmetric. To visualize this asymmetry, we differentially labeled the left and right Hb with DiA and DiO. The left rft (DiA, green; Fig. 3B) singly crossed the midline first and then met the right rft on the right side (DiI, red; Fig. 3B). After this both tracts projected anteriorly together. With the aim to visualize more clearly the rostral trajectory of these tracts in the *Gli2* mutant, we labeled differentially the Hb in an E13.5 mutant embryo prepared as an open neural tube explant (ONT; Fig. 3D, D′). We found that initially the axons of both rft navigated ventrally. The left rft (green) crossed the midline and joined the right rft (red); the resulting aberrant tract turned and proceeded rostralward at the right side (Fig. 3D, D′; compare with the wt, Fig. 2F, F′). We summarized the disrupted trajectory of the rft in the *Gli2* mutant in a schema representation, emphasizing the asymmetric crossing of axons and the antero-posterior mis-direction (Fig. 3E). The

observed phenotype suggests that the floor plate plays an essential role at least in two aspects of the rft guidance at this decision point: midline repulsion and caudalward growth.

The expression pattern of *Slits* is affected in *Gli2* mutant

Robo-Slit signaling is one of the main mechanisms producing midline repulsion of axonal tracts. Simultaneously, *Ntn1*-DCC signaling is the main mechanism for attraction to the midline. We know that in the *Gli2* mutant the expression pattern of the *Slit factors* and *Ntn1* is affected in caudal parts of the central nervous system (Charron et al., 2003; Kadison et al., 2006; Farmer et al., 2008). Therefore, we checked whether *Slit1, Slit2* and *Ntn1* are expressed in the wildtype floor and basal plate of p2 and p1, compared with the corresponding abnormal median basal plate present in the *Gli2* mutant (Figs. 4A, B). In the wildtype, *Ntn1* was expressed in the ventricular zone all along the basal and floor plates (Fig. 4C). In the mutant, *Ntn1* was still strongly expressed in the median basal plate, though the expression was scattered in the area where the tracts met (arrow in Fig. 4D). *Slit*1 was also strongly expressed in the wildtype basal and floor plates (Fig. 4E). Its expression was strongly reduced in the *Gli2* mutant (arrow in Fig. 4F). The wildtype expression of *Slit2* was restricted to the floor plate (Fig. 4G) and in the mutant it was reduced and scattered in the area where the two tracts met (arrow in Fig. 4H). *Slit3* was not mapped since we know that it is not expressed in the floor plate of p2 during the time period when the axons avoid the midline (Farmer et al., 2008).

The observed alterations in the expression of the molecules analyzed are consistent with the aberrant phenotype presented in the *Gli2* mutant. The residual expression of *Ntn1* probably is sufficient to attract the axons ventralwards and the reduced midline expression of *Slit1/2* is then allows the aberrant crossing of the habenular fibers. However, it remains unclear why the aberrant mixed tract of the mutant grows largely rostralwards, a behavior only shown by a minority of wildtype rft axons. Perhaps the vicinity with the wildtype floor plate increases the sensibility of habenular axons to caudal attractants.

Slit2 is the main repulsive cue for the rft axons

We next focused on demonstrating the repulsive role of the Slits and investigated whether either *Slit1* or *Slit2*, or both, were responsible for this effect. We confronted Hb explants with COS cells expressing *Slit1* or *Slit2*, (or control GFP-transfected COS cells) in a Matrigel matrix. When the habenular explants were challenged with *Slit2*-expressing cells, the fibers showed a strong repulsion compared with the control experiment (Fig. 5A, B, D). In contrast, such repulsion did not occur in presence of *Slit1*-expressing cells (Fig. 5C, D). The quantification of this repulsive phenomenon showed that this difference was statistically significant (Fig. 5D). We confirmed our in vitro results analyzing the loss of function of these molecules in mice null for *Slit1* and in double *Slit1/Slit2* nulls. The *Slit1* null embryos showed no rft phenotype; as in the wildtype, the Hb axons were not able to enter the floor plate (Fig. 5E). However, in the double *Slit1/Slit2* null specimens, the strongly DCC-positive habenular fibers were observed to cross from the left side of the brain into the right side (arrow Fig. 5F; compare with the wt, Fig. 1C). This is the same asymmetric behavior observed in *Gli2* mutants lacking a floor plate. Therefore, we confirmed in vivo and in vitro the role of *Slit2* as a specific strongly repulsive cue for the navigating rft axons (particularly

for those of the left side). Our data suggest that *Slit1* either is not involved, or collaborates indirectly with *Slit2*, which is required in the repulsion of Hb axons by the floor plate.

Robo1 mediates *Slit2* repulsion of the rft

Once we identified the ligand responsible for the midline repulsion, we investigated the receptor involved. We studied the expression pattern of the *Slit* receptors (*Robo1* and *Robo2*; Brose et al., 1999; Li et al., 1999) during habenular development. We found that *Robo1* is strongly expressed in the mHb (Fig. 6A, A′), while *Robo2* was weakly expressed (Fig. 6B, B′). High expression levels correlated with the precise moment when the rft axons are being repulsed by the floor plate. We also confronted Hb explants from *Robo1*$^{+/-}$ and *Robo1*$^{-/-}$ embryos with *Slit2*-transfected COS cells. In *Robo1*$^{+/-}$ tissue, the axons were clearly repulsed from the source of *Slit2* (Fig. 6C), whereas *Robo1*$^{-/-}$ axons did not respond to the repulsive signal (Fig. 6D). The quantification of the repulsive effect was statistically significant (Fig. 6E). To confirm *Robo1* function in vivo, we studied the rft of the *Robo1*$^{-/-}$ embryos. The DCC-positive axons entered directly into the floor plate (arrow in Fig. 6F; compare with the wt, Fig. 1C). In contrast, the *Robo2*$^{-/-}$ mouse did not display any abnormal phenotype in the rft (Fig. 6G). The *Robo1*$^{-/-}$ phenotype was clearly confirmed by labeling differentially with DiI and DiA the habenular nuclei in a *Robo1*$^{-/-}$ ONT (Fig. 6H). Both tracts behaved similarly. As they approached the floor plate, the axons defasciculated and entered progressively into the floor plate as the tract proceeded into its caudalward trajectory (Fig. 6H′; compare with the wt, Fig. 2F′). Therefore, our results indicate that *Robo1* is necessary and sufficient to mediate the midline *Slit2-mediated* repulsion of the habenular axons, whereas *Robo2* is not involved in this process.

Discussion

In the present study, we first described the mode and timing by which the Hb axons that constitute the rft make a major pathfinding decision as they eschew crossing the diencephalic midline floor and change from their initial dorsoventral course into an ipsilateral rostrocaudal trajectory that leads them into several rostral hindbrain targets. We next found that in the absence of the floor plate an aberrant mixed rft grows rostralward into the hypothalamus after an asymmetric crossing of the midline. We determined that the absence of *Slit2* is the signaling floor plate-derived cue responsible of this abnormal crossed hypothalamopetal phenotype. We also identified the *Robo1* receptor as the sole partner for *Slit2* in mediating this repulsion from the floor plate.

Trajectory and development of the rft

The distribution of various guidance molecules in time and space is one of the essential elements to be considered for understanding examples of axonal pathfinding. A precise morphological description in space and time of the embryonic development of the tract to be studied is a fundamental prerequisite, particularly when earlier descriptions have introduced a measure of confusion, as is the case of the retroflex tract. Our preliminary analysis employing the prosomeric model as an interpretive paradigm allowed us to conclude that the tract is truly topologically flexed caudalwards at 90 degrees (as interpreted by classic neuroanatomists) at the basal plate of prosomere 2 (thalamic tegmentum). From there the

tract courses strictly longitudinally across the medial tegmentum of prosomere 1 (pretectum) and midbrain, in order to reach final targets in the rostral hindbrain (isthmus and r1). The literature contains frequent reference to an oblique straight course of this tract from the dorsal habenula into the ventral interpeduncular complex, alluding to the observable adult configuration (Fig. 1A). This erroneous concept results from using the alternative (now obsolete) columnar model of Herrick (1910), which does not acknowledge the hairpin-shaped cephalic flexure and misidentifies both the pretectum and the rostral hindbrain as parts of the midbrain (see Dong, 2008). It was thus thought plausible within the columnar conception that habenular axons coursed directly from the dorsal caudal diencephalon (the habenula) into the ventral caudal midbrain (the interpeduncular complex). Nowadays, substantial genoarchitectonic and experimental evidence has accrued supporting the prosomeric boundaries entered in Figure 1A, which imply that the rft course extending beyond the point where the tract approaches the floor plate is strictly longitudinal, and orthogonal to its earlier strictly dorsoventral course within prosomere 2. The cephalic flexure is the morphogenetic cause that this change of direction is not readily apparent. Obviously the assumptions about guidance possibilities for the rft are rather different depending whether the columnar or prosomeric models are employed in the preliminary analysis. The columnar model suggests an oblique straight course, whereas the prosomeric model indicates a change of course with orthogonal limbs. No evidence so far supports oblique straight axonal courses in the brain, and there is much evidence of orthogonal relationships. We concentrated our attention on the retroflexion of the rft relative to prosomeric boundaries, which simultaneously implies a lack of crossing of the local midline.

The trajectory of the rft apparently requires taking at least three decisions. Between E9.5 and E11.5, the rft axons sort out from the habenular area, fasciculating together and growing strictly ventralwards until they reach the p2 basal plate. This initial part of the course is known to be controlled by repulsive signals located in the alar plate of p1 and p2 (*Sema3F* and *Sema5A*, Funato et al., 2000; Kantor et al., 2004), which establish a narrow permissive corridor in front of the pretectum, complemented by an attractive signal from basal p2 (*Ntn1*, Funato et al., 2000). At E11.5, the pioneering Hb axons reach the proximity of the floor plate, but, making a second pathfinding decision, they do not cross it and instead start navigating caudalwards. By E13.5, the rft is distinctly thicker, and the Hb axons arrive at the rostral hindbrain (isthmus and r1), where they make final targeting decisions; e.g., in the case of mHb axons this implies crossing and recrossing several times the local midline as they innervate the IP. At this stage some scattered rft axons do cross the p2 floor plate. Finally, a few rft axons normally project rostralward and innervate a hypothalamic nucleus (Kiss et al., 2002). The rft trajectory underlines the importance of the floor plate in its pathfinding from the locus where it changes its initial course to its end in the hindbrain. Therefore, we aimed our efforts to understand better its role.

Role of the floor plate in the guidance of the rft

The floor plate secretes different molecules that attract or repel diverse axonal tracts (Colamarino and Tessier-Lavigne, 1995; Tessier-Lavigne and Goodman, 1996; Kaprielian et al., 2001). Therefore, we first checked whether this structure is needed for the lack of penetration of the p2 floor plate and the subsequent retroflexion of the rft. The absence of

the floor plate in *Gli2* null mice clearly produced a strong alteration in the trajectory of the rft. The axons correctly grew dorsoventrally, but when they arrived at the p2 basal plate (which is continuous across the abnormal midline) they collected into an aberrant semicrossed tract, which navigated rostralward. Furthermore, under these conditions the axons did not show evidence of any midline-derived repulsion and crossed jointly the midline several times until they arrived at the rostral hypothalamus. Strikingly, the observed aberrant merging of the two tracts was asymmetric. The left rft always crossed singly the midline before meeting and mixing with the right rft. Subsequently both tracts navigated together, crossing several times the midline, until they reached the rostral hypothalamus. We discuss below a plausible explanation for this phenomenon.

Altered guidance molecules in absence of the floor plate

The floor plate expresses repulsive molecules of the *Slit* family (Long et al., 2004) and attractive cues such as *Ntn1* (Kennedy et al., 1994). In the *Gli2* mutant, it is already known that the expression pattern of Slit factors is affected in the caudal central nervous system (Kadison et al., 2006; Farmer et al., 2008). At the embryonic time window of interest for us, *Slit1* and *Slit2* are both expressed in the p2 floor plate. *Slit3* is also expressed in this area, but only later on in development. Our observations indicated that the expression of these molecules is also diminished at basal p2 and p1 domains in the *Gli2* mutant. *Ntn1-DCC* interaction strongly attracts the Hb axons ventralwards (Funato et al., 2000). The expression of *Ntn1* is also altered in *Gli2* mutants, but its persistent low signal levels may be sufficient to attract the rft towards the basal plate. Alternatively the basal plate may express other redundant attractants, or the repulsive effects exerted by the p2 and p1 alar plates may be sufficient to make the rft approach the ventral midline. At midbrain levels the *Ntn1* expression is heavily affected; this finding may serve to explain the aberrant rostral trajectory of the rft axons in the *Gli2* null mutant. It may be also relevant to understand why the rft mainly bends caudalwards in the wildtype.

Slit2 is the essential signal to prevent the entry of the Hb axons into the midline

Slit2, but not *Slit1*, acts as a repellent in interaction with the Hb axons, as we showed using *in vitro* and *in vivo* experiments. The *Slit1* loss of function mice did not present any alteration in the trajectory of the rft. In the absence of both Slits, the left rft crossed abnormally over the midline and joined the right rft, just as in the *Gli2* phenotype. In contrast, in this case the joined tracts navigated caudalwards and re-crossed the midline when they arrived at their IP target. These results indicate that *Slit2* is the main midline repellent for the Hb axons. One striking result is that the axons entering the floor plate did not stall there, and were able to exit the midline contralaterally. Therefore the axons probably have the capability to react to other repulsive cues from the floor plate, or are rendered there preferentially attracted by basal plate signals. Furthermore, the joined tract coursing on the right side navigated caudalward and did not re-cross the floor plate until it arrived at the normal midline crossing domain in r1. Nevertheless, this r1 crossing is also severely altered in this mutant. Surprisingly, altering *Slit2* in addition to *Slit1* produced the same asymmetric effect as we observed before. The causes of this asymmetry remain obscure.

Robo1 mediates the repulsion of the Hb axons

Robo1 and *Robo2* are the main receptors that mediate the repulsion effects generated by the Slits in several axonal systems (Long et al., 2004; Farmer et al., 2008; Lopez-Bendito et al., 2007). The *Robo* expression pattern analysis in the Hb showed that *Robo1* is strongly expressed in the mHb during embryonic development. However, *Robo2* is also weakly expressed at early stages. In the absence of *Robo1*, the habenular axons were able to enter the floor plate. Our explants showed that this is due to the lack of the capability to respond to *Slit2*. In contrast, in the absence of *Robo2* the axons were still repelled by the midline floor.

In *Robo1* loss of function mice, the phenotype was less severe than in the *Slit1/2* double mutant. The number of axons that crossed the midline was lower than in the *Slit1/2* mutant. The stronger phenotype of the ligand compared with the receptor indicates that there may be other receptors participating in this repulsive mechanism. Once again, the fact that the *Robo1* mutant axons did not stall in the floor plate indicates that they maintain a capability to sense other repulsive signals from the floor plate.

All these data reveal that the midline repulsion of the Hb axons is a complex process in which Slit2 is the main repellent. There may exist accessory repulsive cues that apparently force the axons to exit the floor plate after entering it, in absence of the major Slit2 effect. The rft is a heterogeneous bundle of axons, in which *Robo1* mediates the repulsion of mHb axons but no the lHb. However the full tract reacts to the lack of *Slit2*, therefore possibly implying that the lHb may express a still unknown receptor for *Slit2*. We did not address the mechanisms that allow the mHb axons to cross and re-cross the floor plate when they reach r1. A plausible candidate to control this phenomenon is possibly *Robo3*, since the spliced form *Robo3.1* allows commissural axons to suppress the repulsion from midline Slits (Chen et al., 2008).

Asymmetric phenotype

In the absence of a floor plate (*Gli2*$^{-/-}$) and separately in the *Slit1/2* loss of function we constantly obtained a striking asymmetric phenotype in the rft trajectory. In both cases, the left rft singly crossed the midline and joined the right rft, fasciculating with it. The resulting aberrant tract grew rostralward into the hypothalamus on the right side of the brain in the absence of floor plate, re-crossing several times the midline. In contrast, the aberrant rft in the *Slit1/2* lack of function embryos displayed a caudalward trajectory on the right side and did not re-cross the midline.

In lower vertebrates, the Hb nuclei show a strong asymmetry. The left Hb is usually much bigger than the right Hb (Concha and Wilson, 2001; Bianco and Wilson, 2009). This difference in size is also visible in the rft. A plausible explanation for our asymmetric phenotypes is that the alterations in the floor and basal plates have unveiled that the apparently symmetric Hb complexes of the mouse hide an asymmetric molecular profile. The modification of the local basal territories may have produced an asymmetric distribution of attractive cues, so that the right side results more attractive. The normal generation of attractive signals by the basal plate may be influenced by the presence of *Slit2*.

In conclusion, the rft displays a complex trajectory across several neuromeres, whose causal explanation requires investigation of three main pathfinding decision points (sorting dorsoventrally out of the habenula, retroflexion at basal p2, with consequent longitudinal growth caudalward across the p1 and midbrain tegmentum, and final zig-zagging across the medioventral IP complex in r1). In the literature, this trajectory has been usually misinterpreted due to disregarding the somewhat cryptic cephalic flexure of adult brains and accepting the now obsolete columnar view of the midbrain as extending from the rft all the way to the pons. We examined the retroflexion behavior and learned that a floor plate-related *Robo1-Slit2* signaling mechanism is responsible for this crucial navigational decision. Our prosomeric interpretation of the trajectory of this tract, and its sequentially changing circumstances clearly opens the possibility to interpret within the same robust causal scenario further phenotypes obtained in other signaling mutants both as regards both the development of the rft and of many other tracts.

Material & Methods

Mouse strains

The day when the vaginal plug was detected was considered as embryonic day 0.5 (E0.5). All mouse manipulation and experimental procedures were performed according to the directives of the Spanish and European Union governments and protocols approved by the Universidad Miguel Hernandez CEIE Animal Experimentation Committee. Breeding and collection of *Robo* and *Slit* mutant mice were carried out under the approval of the IACUC of the University of Nevada, Reno.

***-Pou4f1* tau-lacZ strain—**The *Pou4f1* tau-LacZ strain was kindly provided by Dr. Eric E. Turner (Seattle Children's Research Institute). A transgene encoding tau-linked-LacZ is located under the *Pou4f1* promoter (Quina et al., 2005). The cells expressing *Pou4f1* produce the enzyme galactosidase, which appears in the cell body and axonal projections due to the associated TAU protein.

***-Gli2*^{zfd} mutant mice—**The *Gli2*$^{-/-}$ mutants embryos (n=10) were obtained by crossing *Gli2*$^{+/-}$ parents maintained in a C57BL/6J background. The genotyping of the *Gli2*^{ZFD} allele was as described previously (Mo et al., 1997).

Robo and *Slit* mutant mice

The *Robo1*$^{-/-}$ (n=18), *Robo2*$^{-/-}$ (n=10), *Slit1*$^{-/-}$ (n=4); and *Slit1*$^{-/-}$, *Slit2*$^{-/-}$ (n=3) double mutant mice used were genotyped as previously described (Grieshammer et al., 2004; Long et al., 2004; Lopez-Bendito et al., 2007).

Enzymatic Staining

For (β-galactosidase activity staining, an adult mouse was perfused with 2% paraformaldehyde (PFA) in PBS. 100μm vibratome sections were stained by incubation in X-gal solution at 37 °C overnight. The X-gal solution is contains 1mg/ml Xgal, 2mM $MgCl_2$, 20mM Fe^{2+} and 20mM Fe^{3+} in PBS.

In Situ Hybridization (ISH) and Immunohistochemistry (IHC)

For ISH, mouse brains were fixed overnight in 4% PFA in PBS. 7μm paraffin sections were hybridized with the following digoxigenin-labeled probes: *Netrin-1* (O. Reiner), *Slit1*, *Slit2*, *Slit3*, *Robo1* and *Robo2* (O. Marín). Paraffin or vibratome sections were used for α-DCC IHC (1:100; Santa Cruz #sc-6535). In both cases the protocols were as previously described (Moreno-Bravo et al., 2013).

Open Neural Tube Explant Technique (ONTs)

Timed pregnant mice were killed by cervical dislocation and embryos were dissected in cold 1x PBS. Heads from E11.5 and 13.5 embryos were cut off at the level of r2, and the mesenchyme and epidermis were removed. The neural tube was opened along the dorsal midline in a caudal to rostral direction. The telencephalic vesicles and hypothalamus regions were eliminated, in order to obtain a flat tissue. The regions surrounding the area where the rft develops were kept intact. Finally the dissected neural tube preparations were cultured like an open book with the pial surface contacting a polycarbonate membrane (MilliCell PICMORG50). It was possible to recognize the diencephalic prosomeres (p1, p2 and p3), the midbrain and isthmus/r1 region.

Axonal tracing

For axonal tracing, the ONTs were fixed for 1hour in 4% PFA. Small DiI crystals (1,1′-dioctadecyl 3,3,3′,3′-tetramethylindocarbo-cyanine perchlorate; Molecular Probes) or DiA crystals (4–4-dihexadecyl aminostyryl N-methyl-pyridinium iodide; Molecular Probes) were inserted into the habenular nuclei. The labeled ONTs were incubated at 37°C in 4% PFA until the tracers had diffused sufficiently. DAPI (4′, 6-Diamidino-2-Phenylindole, dihydrochloride; Sigma #D9542) was used as a fluorescent nuclear counterstain.

Matrigel Co-culture

E12.5 mouse brain tissue was dissected in ice-cold 1x Krebs. The Hb area was dissected out from an ONT. COS7 cells were transfected by lipofection (Lipofectamine 2000 reagent, Invitrogen) of a *Slit1* (M. Tessier-Lavigne), *Slit2*-myc (G. Mastick) or GFP-expressing vector (PCX-GFP; A. Nieto) and cultured for 24h. Aggregates of COS7 transfected cells were prepared by embedding transfected cells in Matrigel. (BD Biosciences, Franklin Lakes, NJ, USA)

The Hb explants were placed on top of Matrigel drops, confronted to the aggregate of transfected cells, and covered with diluted Matrigel in Neurobasal culture medium (1:1; Gibco Life Technologies). The co-cultures were incubated for up to 48h in Neurobasal medium supplemented with 1x B-27, 25mM glucose, 2mM glutamine and 100U/ml pen-strep (Invitrogen).

After the incubation, the explants were fixed with 4% PFA and labeled with a small DiI crystal. Each explant was divided in two 45 degree quadrants, proximal or distal to the COS7 aggregate. The axon lengths were summed within each quadrant and the ratio between proximal and distal length was calculated. To compare the mean ratios between

control GFP and *Slit1* or *Slit2* transfections, the test of Student or of Mann-Whitney were used, depending on the distribution of the data (SigmaStat software).

Acknowledgments

We thank to E. Turner for kindly provided the Pou4f1-TauLacZ transgenic line. We are also grateful to O. Marín for providing the Robo1, Robo2, Slit1, Slit2, Slit3 probes; O. Reiner for provide Netrin1 probe; M. Tessier-Lavigne for providing the Slit1 functional construct and A. Nieto for providing the PCX-GFP plasmid. We thank E. Leyva-Diaz, R. Susin and C. Merino from Lopez-Bendito lab for helping us in the generation and genotyping of the Robo transgenic embryos. We are also grateful with E. Domiguez and A. Sempere for statistical advice, L. Puelles and S. Martínez lab, especially D. Echevarría, for helpful discussions and comments.

Funding

Work supported by “Ministerio de Economía y Competitividad” BFU2010-16548 (FEDER Fonds) to E. Puelles, BFU2012-34298 to G. Lopez-Bendito; Consolider Grant (CSD2007-00023) and European commission (EUCOMMTOOLS, contract 261492) to S.M. J.A. Moreno-Bravo was supported by the Predoctoral Program of the “Consejo Superior de Investigaciones Científicas-Junta de Ampliación de Estudios”, co-financed by the European Social Fund. Funding was also provided to G.S. Mastick by NIH grants R21NS077169, with core facility support by NIH COBREs 1 P20 RR024210 and 1 P20 GM103650, and the Nevada INBRE 8 P20 GM103440-11.

References

Andres KH, Düring von M, Veh RW. Subnuclear organization of the rat habenular complexes. J Comp Neurol. 1999; 407:130–150. [PubMed: 10213193]

Bagri A, Marín O, Plump AS, Mak J, Pleasure SJ, Rubenstein JLR, Tessier-Lavigne M. Slit proteins prevent midline crossing and determine the dorsoventral position of major axonal pathways in the mammalian forebrain. Neuron. 2002; 33:233–248. [PubMed: 11804571]

Bianco IH, Wilson SW. The habenular nuclei: a conserved asymmetric relay station in the vertebrate brain. Philos Trans R Soc Lond, B, Biol Sci. 2009; 364:1005–1020. [PubMed: 19064356]

Brose K, Bland KS, Wang KH, Arnott D, Henzel W, Goodman CS, Tessier-Lavigne M, Kidd T. Slit proteins bind Robo receptors and have an evolutionarily conserved role in repulsive axon guidance. Cell. 1999; 96:795–806. [PubMed: 10102268]

Charron F, Stein E, Jeong J, McMahon AP, Tessier-Lavigne M. The morphogen sonic hedgehog is an axonal chemoattractant that collaborates with netrin-1 in midline axon guidance. Cell. 2003; 113:11–23. [PubMed: 12679031]

Chen Z, Gore BB, Long H, Ma L, Tessier-Lavigne M. Alternative splicing of the Robo3 axon guidance receptor governs the midline switch from attraction to repulsion. Neuron. 2008; 58:325–332. [PubMed: 18466743]

Colamarino SA, Tessier-Lavigne M. The role of the floor plate in axon guidance. Annu Rev Neurosci. 1995; 18:497–529. [PubMed: 7605072]

Concha ML, Wilson SW. Asymmetry in the epithalamus of vertebrates. J Anat. 2001; 199:63–84. [PubMed: 11523830]

Devine CA, Key B. Robo-Slit interactions regulate longitudinal axon pathfinding in the embryonic vertebrate brain. Dev Biol. 2008; 313:371–383. [PubMed: 18061159]

Ding Q, Motoyama J, Gasca S, Mo R, Sasaki H, Rossant J, Hui CC. Diminished Sonic hedgehog signaling and lack of floor plate differentiation in Gli2 mutant mice. Development. 1998; 125:2533–2543. [PubMed: 9636069]

Dong, HW. The Allen Reference Atlas: A Digital Color Brain Atlas of the C57BL/6J Male Mouse. The Allen Institute for Brain Science/Wiley & Sons; 2008.

Farmer WT, Altick AL, Nural HF, Dugan JP, Kidd T, Charron F, Mastick GS. Pioneer longitudinal axons navigate using floor plate and Slit/Robo signals. Development. 2008; 135:3643–3653. [PubMed: 18842816]

Funato H, Saito-Nakazato Y, Takahashi H. Axonal growth from the habenular nucleus along the neuromere boundary region of the diencephalon is regulated by semaphorin 3F and netrin-1. Mol Cell Neurosci. 2000; 16:206–220. [PubMed: 10995548]

Geisler M, Trimble M. The Lateral Habenula: No Longer Neglected. CNS Spectr. 2008; 13:484–489. [PubMed: 18567972]

Grieshammer U, Le Ma, Plump AS, Wang F, Tessier-Lavigne M, Martin GR. SLIT2-mediated ROBO2 signaling restricts kidney induction to a single site. Dev Cell. 2004; 6:709–717. [PubMed: 15130495]

Herrick CJ. The evolution of the intelligence and its organs. Science. 1910; 31:7–18. [PubMed: 17758520]

Hong S, Hikosaka O. The globus pallidus sends reward-related signals to the lateral habenula. Neuron. 2008; 60:720–9. [PubMed: 19038227]

Hong S, Jhou TC, Smith M, Saleem KS, Hikosaka O. Negative reward signals from the lateral habenula to dopamine neurons are mediated by rostromedial tegmental nucleus in primates. J Neurosci. 2011; 31:11457–71. [PubMed: 21832176]

Kadison SR, Murakami F, Matise MP, Kaprielian Z. The role of floor plate contact in the elaboration of contralateral commissural projections within the embryonic mouse spinal cord. Dev Bio. 2006; 296:499–513. [PubMed: 16854408]

Kantor DB, Chivatakarn O, Peer KL, Oster SF, Inatani M, Hansen MJ, Flanagan JG, Yamaguch Y, Sretavan DW, Giger RJ, Kolodkin AL. Semaphorin 5A is a bifunctional axon guidance cue regulated by heparan and chondroitin sulfate proteoglycans. Neuron. 2004; 44:961–975. [PubMed: 15603739]

Kaprielian Z, Runko E, Imondi R. Axon guidance at the midline choice point. Dev Dyn. 2001; 221:154–181. [PubMed: 11376484]

Kastenhuber E, Kern U, Bonkowsky JL, Chien C, Driever W, Schweitzer J. Netrin-DCC, Robo-Slit, and heparan sulfate proteoglycans coordinate lateral positioning of longitudinal dopaminergic diencephalospinal axons. J Neurosci. 2009; 9:8914–8926. [PubMed: 19605629]

Kennedy TE, Serafini T, La Torre de JR, Tessier-Lavigne M. Netrins are diffusible chemotropic factors for commissural axons in the embryonic spinal cord. Cell. 1994; 78:425–435. [PubMed: 8062385]

Kim M, Roesener AP, Mendonca PRF, Mastick GS. Robo1 and Robo2 have distinct roles in pioneer longitudinal axon guidance. Dev Biol. 2011; 358:181–188. [PubMed: 21820427]

Kiss J, Csáki A, Bokor H, Kocsis K, Kocsis B. Possible glutamatergic/aspartatergic projections to the supramammillary nucleus and their origins in the rat studied by selective [(3)H]D-aspartate labelling and immunocytochemistry. Neuroscience. 2002; 111:671–691. [PubMed: 12031353]

Klemm WR. Habenular and interpeduncularis nuclei: shared components in multiple-function networks. Med Sci Monit. 2004 Nov.10:RA261–73. [PubMed: 15507867]

Lecourtier L, Kelly PH. A conductor hidden in the orchestra? Role of the habenular complex in monoamne transmission and cognition. Neurosci Biobehav Rev. 2007; 31:658–72. [PubMed: 17379307]

Li HS, Chen JH, Wu W, Fagaly T, Zhou L, Yuan W, Dupuis S, Jiang ZH, Nash W, Gick C, Ornitz DM, Wu JY, Rao Y. Vertebrate slit, a secreted ligand for the transmembrane protein roundabout, is a repellent for olfactory bulb axons. Cell. 1999; 96:807–818. [PubMed: 10102269]

Long H, Sabatier C, Ma L, Plump A, Yuan W, Ornitz DM, Tamada A, Murakami F, Goodman CS, Tessier-Lavigne M. Conserved roles for Slit and Robo proteins in midline commissural axon guidance. Neuron. 2004; 42:213–223. [PubMed: 15091338]

López-Bendito G, Flames N, Ma L, Fouquet C, Di Meglio T, Chédotal A, Tessier-Lavigne M, Marín O. Robo1 and Robo2 cooperate to control the guidance of major axonal tracts in the mammalian forebrain. J Neurosci. 2007; 27:3395–3407. [PubMed: 17392456]

Matise MP, Epstein DJ, Park HL, Platt KA, Joyner AL. Gli2 is required for induction of floor plate and adjacent cells, but not most ventral neurons in the mouse central nervous system. Development. 1998; 125:2759–2770. [PubMed: 9655799]

Mo R, Freer AM, Zinyk DL, Crackower MA, Michaud J, Heng HH, Chik KW, Shi XM, Tsui LC, Cheng SH, Joyner AL, Hui C. Specific and redundant functions of Gli2 and Gli3 zinc finger genes in skeletal patterning and development. Development. 1997; 124:113–123. [PubMed: 9006072]

Moreno-Bravo JA, Perez-Balaguer A, Martinez-Lopez JE, Aroca P, Puelles L, Martínez S, Puelles E. Role of Shh in the development of molecularly characterized tegmental nuclei in mouse rhombomere 1. Brain Struc Funct. 201310.1007/s00429-013-0534-6

Morgane PJ, Galler JR, Mokler DJ. A review of systems and networks of the limbic forebrain/limbic midbrain. Prog Neurobiol. 2005; 75:143–60. [PubMed: 15784304]

Plum AS, Erskine L, Sabatier C, Brose K, Epstein CJ, Goodman CS, Mason CA, Tessier-Lavigne M. Slit1 and Slit2 cooperate to prevent premature midline crossing of retinal axons in the mouse visual system. Neuron. 2002; 33:219–232. [PubMed: 11804570]

Puelles L, Rubenstein JLR. Forebrain gene expression domains and the evolving prosomeric model. Trends Neurosci. 2003; 26:469–476. [PubMed: 12948657]

Puelles, L.; Martínez-de-la-Torre, M.; Ferran, JL.; Watson, C. Diencephalon. In: Watson, C.; Paxinos, G.; Puelles, L., editors. The mouse nervous system. San Diego: Elsevier Academic Press; 2012. p. 313-336.

Quina LA, Pak W, Lanier J, Banwait P, Gratwick K, Liu Y, Velasquez T, O'Leary DDM, Goulding M, Turner EE. Brn3a-expressing retinal ganglion cells project specifically to thalamocortical and collicular visual pathways. J Neurosci. 2005; 25:11595–11604. [PubMed: 16354917]

Ramón y Cajal A. Histologie du système nerveux de l'homme & des vertébrés. 1909; I

Ricaño-Cornejo I, Altick AL, García-Peña CM, Nural HF, Echevarria D, Miquelajáuregui A, Mastick GS, Varela-Echavarría A. Slit-Robo signals regulate pioneer axon pathfinding of the tract of the postoptic commissure in the mammalian forebrain. J Neurosci Res. 2011; 89:1531–1541. [PubMed: 21688288]

Sahay A, Molliver ME, Ginty DD, Kolodkin AL. Semaphorin 3F is critical for development of limbic system circuitry and is required in neurons for selective CNS axon guidance events. J Neurosci. 2003; 23:6671–6680. [PubMed: 12890759]

Sutherland RJ. The dorsal diencephalic conduction system: a review of the anatomy and functions of the habenular complex. Neurosci Biobehav Rev. 1982 Spring;6:1–13. [PubMed: 7041014]

Tessier-Lavigne M, Goodman CS. The molecular biology of axon guidance. Science. 1996; 274:1123–1133. [PubMed: 8895455]

Viswanath H, Carter AQ, Baldwin PR, Molfese DL, Salas R. The medial habenula: still neglected. Front Hum Neurosci. 201410.3389/fnhum.2013.00931

Zhang C, Gao J, Zhang H, Sun L, Peng G. Robo2--slit and Dcc--netrin1 coordinate neuron axonal pathfinding within the embryonic axon tracts. J Neurosci. 2012; 32:12589–12602. [PubMed: 22956848]

Zou Y, Stoeckli E, Chen H, Tessier-Lavigne M. Squeezing axons out of the gray matter: a role for slit and semaphorin proteins from midline and ventral spinal cord. Cell. 2000; 102:363–375. [PubMed: 10975526]

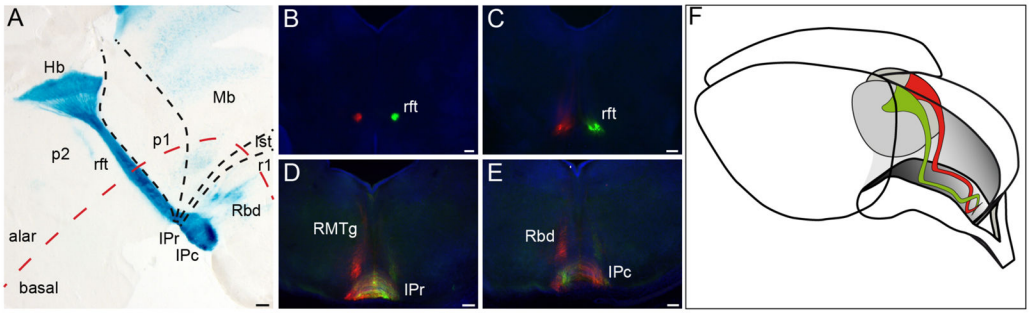

Figure 1. Symmetric trajectory of the rft

(A) Sagittal section of a X-gal-stained *Pou4f1-tauLacZ* adult brain. The black dotted lines define the boundaries between different neuromeres (p2, p1, mb, ist, r1). The red dotted line indicates the alar-basal boundary. (B–E) Coronal sections of an E18.5 embryo, ordered from rostral to caudal levels, showing nuclear staining (DAPI) and differential fluorescent tracing of the two habenular efferent tracts (rft). We inserted DiI (right Hb) and DiA (left Hb) crystals. Abbreviations: IPc, caudal interpeduncular nucleus; IPr, rostral interpeduncular nucleus; Ist, isthmus; Mb, midbrain; p1, prosomere 1 (pretectum); p2, prosomere 2 (thalamus), rft, retroflex tract; RMTg, rostromedial tegmental nucleus r1, rhombomere 1. Scale bar: 200μm.

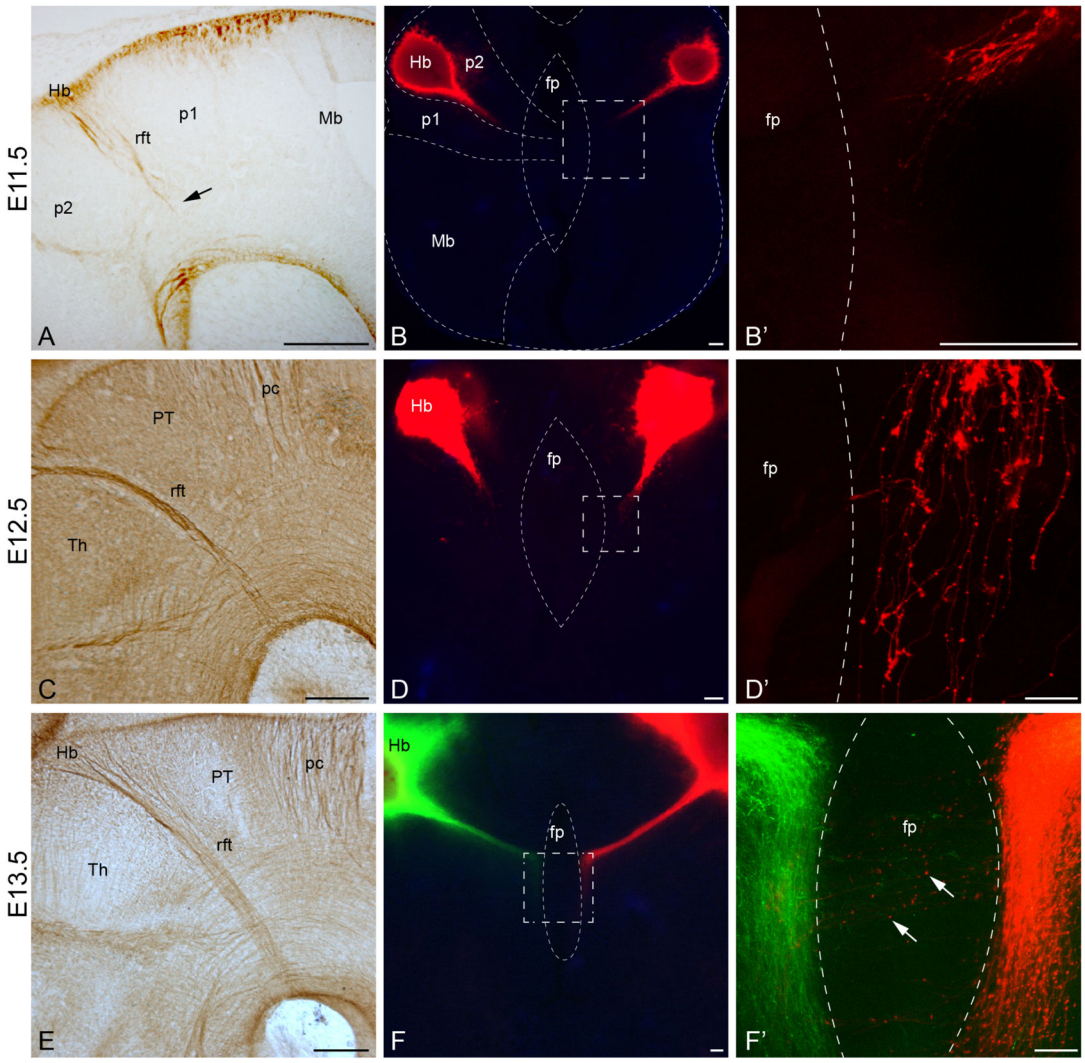

Figure 2. Embryonic development of the rft

(A, C, E) Sagittal sections of E11.5 (A, paraffin), E12.5 (C, vibratome) and E13.5 (E, vibratome) immunoreacted against DCC. (B, D, F) Top view of E11.5 (B), E12.5 (D) and E13.5 (F) ONTs showing DiI and DiA labeling of rft. (B′, D′, F′) Higher magnification images obtained by confocal microscopy of B, D and F (dotted boxed regions). The dotted lines define the border of the ONTs, the boundaries between the prosomeres and the floor plate. The arrows in F′ point to scattered floor plate-crossing axons. Abbreviations: fp, floor plate; Hb, habenula; Ist, Isthmus; Mb, Midbrain; pc, posterior commissure; p1, prosomere1; p2, prosomere2; PT, pretectum; rft, retroflex tract; Th, Thalamus. Scale bar: 200μm and 100μm in F′.

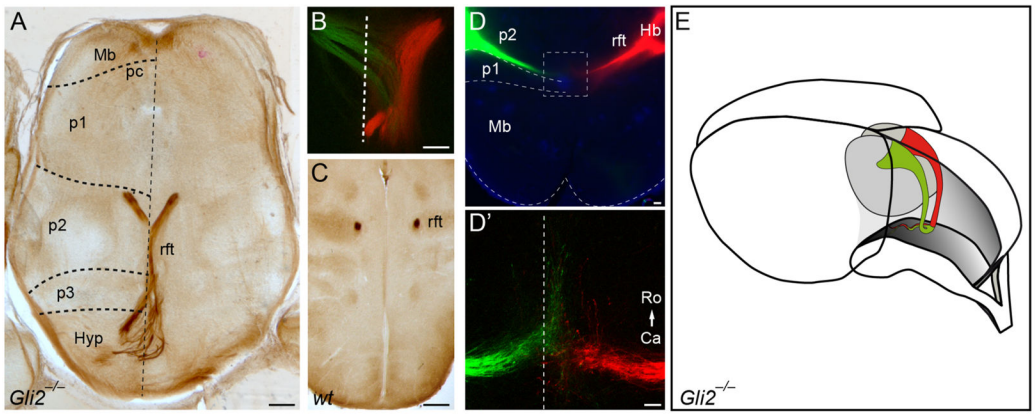

Figure 3. Altered rft trajectory in the *Gli2* mutant

(A) Vibratome horizontal section through midbrain, diencephalon and hypothalamus of an E18.5 *Gli2*$^{-/-}$ embryo stained with α–DCC. This image is the result of the superposition of two consecutive sections, in order to show the overall rostralward trajectory of the aberrant rft tracts. (B) This insert shows a high magnification image of a vibratome coronal section of an E18.5 *Gli2*$^{-/-}$ brain in which the right and left Hb were labeled with DiI (red) and DiA (green), respectively. (C) Vibratome coronal section of an E18.5 *wt* embryo stained with α–DCC. (D) Top view of an E13.5 *Gli2*$^{-/-}$ ONT labeled with DiI (right Hb, red) and DiA (left Hb, green). (D′) Higher magnification of dotted boxed region in (D) obtained by confocal microscopy. E: Schematic diagram showing the altered trajectory of the rft in *Gli2*$^{-/-}$ mice (compare Fig. 1F). The dotted line in (A) and (D) defines the boundaries between the different neuromeres. The dotted line in (B) and (D′) represents the midline. Ca, caudal; Hb, habenula; Hyp, hypothalamus; Ist, Isthmus; Mb, Midbrain; pc, posterior commissure; p1, prosomere1; p2, prosomere2; p3, prosomere 3; ro, rostral; rft, retroflex tract. Scale bar: 200μm and 50 μm in B and D′.

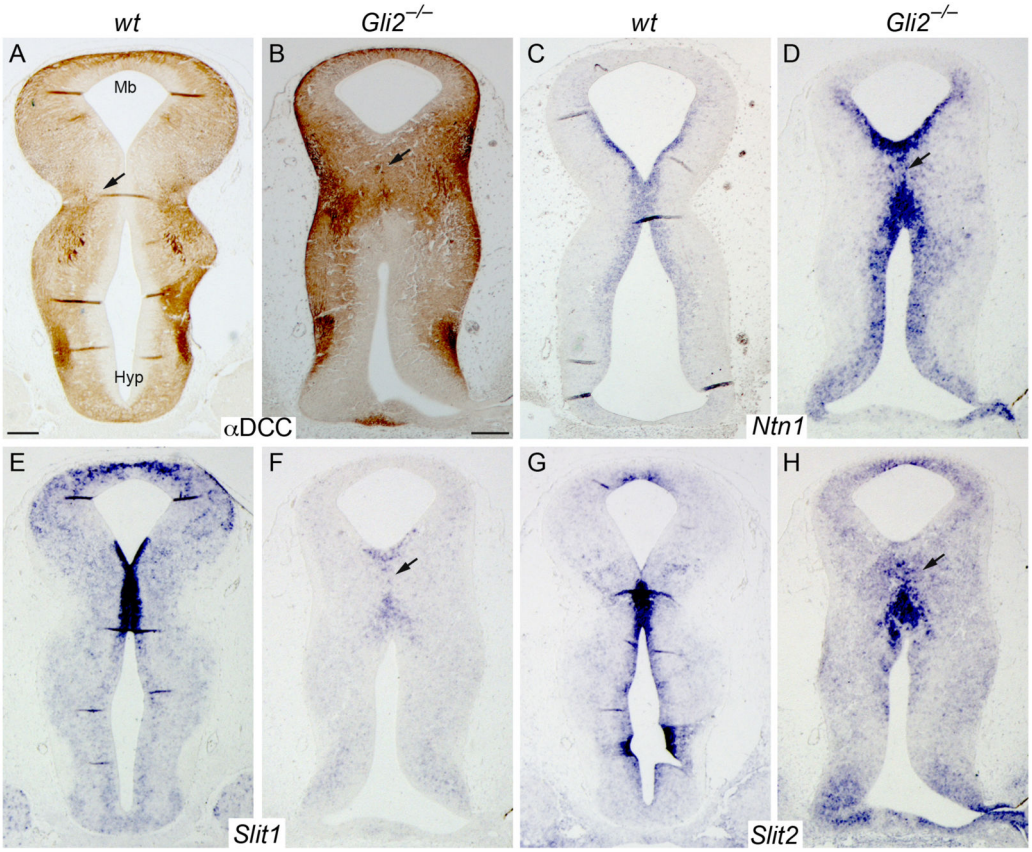

Figure 4. Abnormal expression of signaling cues in *Gli2*$^{-/-}$ embryos

(A–H) Adjacent horizontal paraffin sections of one E12.5 wild type specimen (A, C, E, G) and one *Gli2* mutant embryo (B, D, F, H) at comparable section levels. (A–B) Immunohistochemistry against DCC. (C–H) In situ hybridization for *Ntn1* (C, D), *Slit1* (E, F) and *Slit2* (G, H). The arrows in A and B show the localization of the rft in a wild type embryo (A) and in a *Gli2* mutant (B). The arrow in D, F and H shows the alteration of the expression of these floor plate guidance cues where the rft adopts an abnormal trajectory. Hyp, hypothalamus; Mb, Midbrain. Scale bar: 200μm.

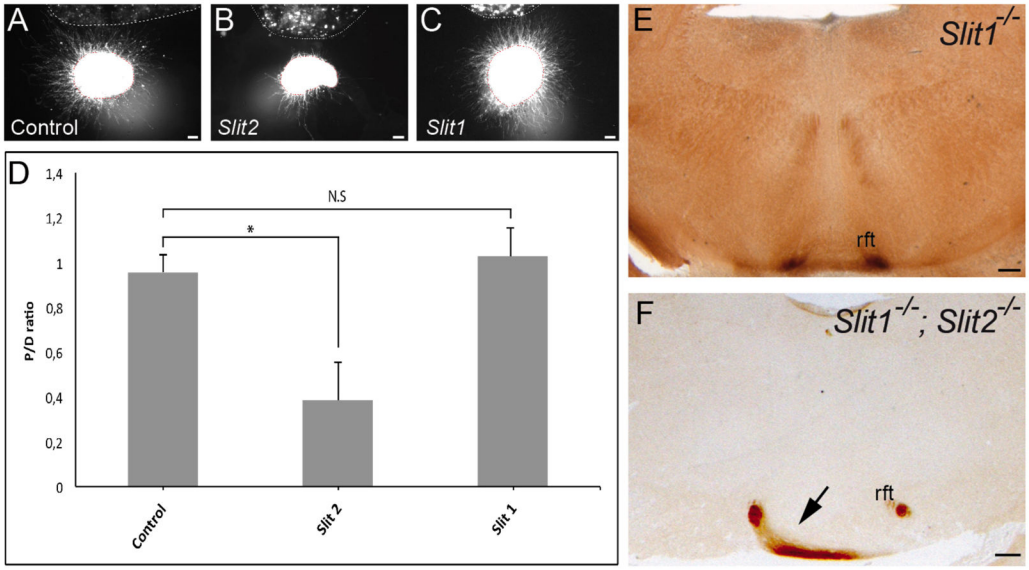

Figure 5. *Slit2* as the main repulsive cue for the rft

(A–C) E12.5 habenular explants were cultured with COS cells expressing GFP (A), *Slit2* (B) or *Slit1* (C). (D) COS cells transfected with GFP (control, 0,954±0,077; n=15) and *Slit1* (1,027±0,1242; n=9) had no repulsive effect on habenular axons. In contrast, the presence of *Slit2* produced a strong repulsion (0,384± 0,173; n=12). For statistical analysis Student's t-test, or Mann-Whitney's test were used, depending on the distribution of the data. Values are given as ± s.d. *p was < 0.001 for *Slit2* compared with control. (E) Vibratome coronal section from an E18.5 *Slit1* mutant embryo labeled against DCC, showing normal rft tracts. (F) Transversal paraffin section from an E18.5 *Slit1-Slit2* double mutant embryo immunolabeled against DCC. The arrow in F indicates the marked crossing of fibers of the left rft to the contralateral side of the brain. Abbreviations: rft, retroflex tract. Scale bar: 200μm.

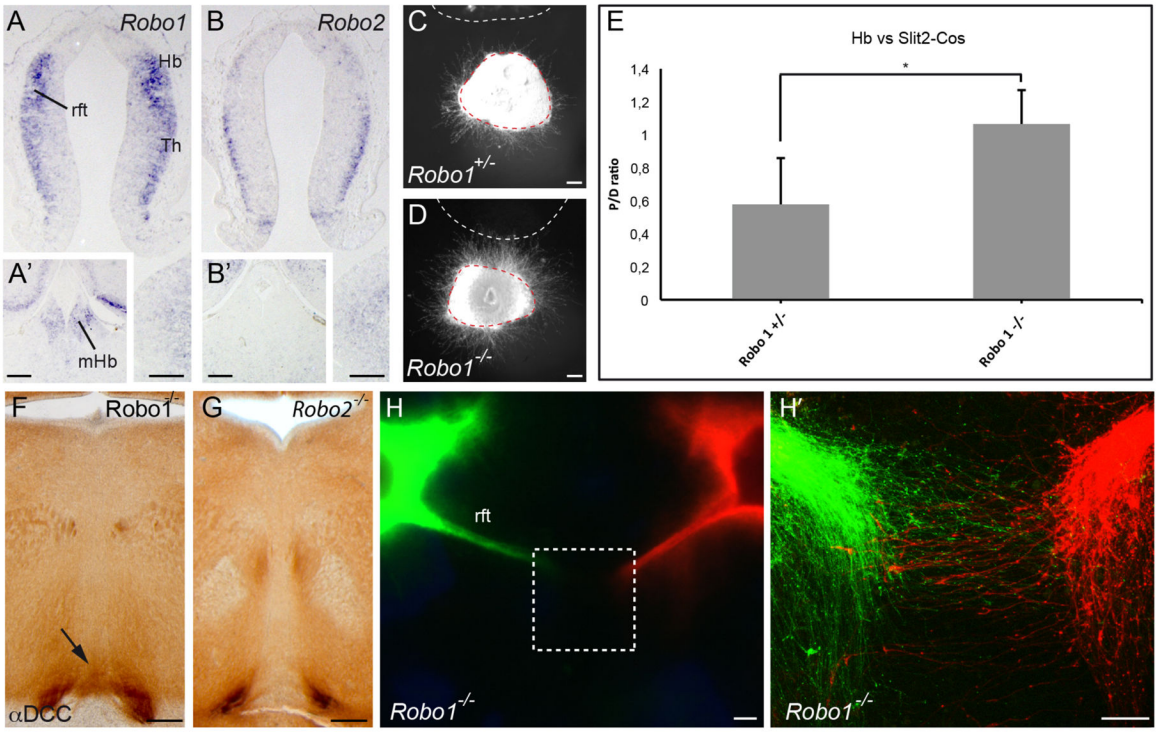

Figure 6. *Robo1* mediates the *Slit2* repulsion of the mHb axons

(A–B) In situ hybridization for *Robo1* (A, A′) and *Robo2* (B, B′) in a paraffin coronal section of an E12.5 (A, B) and E18.5 (A′, B′) embryo, showing expression in the Hb. (C, D) E12.5 Hb explants from *Robo1*$^{+/-}$ (C) and *Robo1*$^{-/-}$ (D) embryos. They were cultured with COS cells expressing *Slit2*. (E) The repulsion of *Slit2* (0,573±0,289, n= 11) disappeared in absence of *Robo1* (1,063±0,204 n= 11). For statistical analysis Student t- test was used. Values are given ± s.d. *p was < 0.001 for *Robo1*$^{-/-}$ compared with *Robo1*$^{+/-}$. (F–G) Vibratome coronal section from an E18.5 *Robo1* (F) and *Robo2* (G) mutant embryo labeled against DCC. The arrow in (F) indicates the presence of DCC labeled axons entering the midline. (H) Top view of an E13.5 *Robo1* mutant ONT labeled with DiI (right Hb, red) and DiA (left Hb, green). (H′) Higher magnification of the boxed region in (H), obtained by confocal microscopy. Abbreviations: Hb, habenula; mHb, medial habenula; rft, retroflex tract; Th, thalamus. Scale bar: 200μm and 100μm in H′.